
Enhancing GNNs Performance on Combinatorial Optimization by Recurrent Feature Update

Daria Pugacheva
JIHT RAS,
pugachyova.d@gmail.com

Andrei Ermakov
HSE University

Igor Lyskov
RMIT

Ilya Makarov
AIRI, MEPhI

Yuriy Zotov
Independent Researcher

Abstract

Combinatorial optimization (CO) problems are crucial in various scientific and industrial applications. Recently, researchers have proposed using unsupervised Graph Neural Networks (GNNs) to address NP-hard combinatorial optimization problems, which can be reformulated as Quadratic Unconstrained Binary Optimization (QUBO) problems. GNNs have demonstrated high performance with nearly linear scalability and significantly outperformed classic heuristic-based algorithms in terms of computational efficiency on large-scale problems. However, when utilizing standard node features, GNNs tend to get trapped to suboptimal local minima of the energy landscape, resulting in low quality solutions. We introduce a novel algorithm, denoted hereafter as QRF-GNN, leveraging the power of GNNs to efficiently solve CO problems with QUBO formulation. It relies on unsupervised learning by minimizing the loss function derived from QUBO relaxation. The proposed key components of the architecture include the recurrent use of intermediate GNN predictions, parallel convolutional layers and combination of static node features as input. Altogether, it helps to adapt the intermediate solution candidate to minimize QUBO-based loss function, taking into account not only static graph features, but also intermediate predictions treated as dynamic, i.e. iteratively changing recurrent features. The performance of the proposed algorithm has been evaluated on the canonical benchmark datasets for maximum cut, graph coloring and maximum independent set problems. Results of experiments show that QRF-GNN drastically surpasses existing learning-based approaches and is comparable to the state-of-the-art conventional heuristics, improving their scalability on large instances.

1 Introduction

Combinatorial Optimization (CO) is a well-known subject in computer science, bridging operations research, discrete mathematics and optimization. Informally, given some ground set, the CO problem is to select the combination of its elements, such that it lies on the problem's feasible domain and the cost of this combination is minimized. A significant amount of CO problems are known to be NP-hard, meaning that they are computationally intractable under " $P \neq NP$ " conjecture and the scope of application for exact algorithms to solve them is very narrow. Therefore, the development of heuristic methods that provide high-accuracy solutions in acceptable amount of time is a crucial challenge in the field Boussaïd et al. [2013].

A wide range of CO problems are defined on structural data, and their solutions are encoded as a subset of graph's edges or nodes. Implicit regularities and patterns often arise in graph structure and

features, making the use of machine learning and especially graph neural networks (GNNs) very promising Cappart et al. [2023].

One notable CO problem is the Quadratic Unconstrained Binary Optimization (QUBO), which aims to minimize a pseudo-Boolean polynomial $\mathcal{F}(x)$ of degree two Hammer and Rudeanu [1969], Boros and Hammer [1991]:

$$\min_{x \in \{0,1\}^n} \mathcal{F}(x) = \sum_{i=1}^n \sum_{j=1}^n x_i A_{ij} x_j + \sum_{i=1}^n c_i x_i = x^T Q x, \quad (1)$$

where the symmetric matrix of coefficients $A \in \mathbb{R}^{n \times n}$ and $c \in \mathbb{R}^n$ encode the initial problem, $x = (x_1, x_2, \dots, x_n)^T$ is the vector of binary variables $x_i \in \{0, 1\}$ and $Q \in \mathbb{R}^{n \times n} = A + \text{diag}(c)$. The latter equivalence in Equation 1 holds because $x_i^2 = x_i$ for all i .

Despite the QUBO problem has been studied for a very long time Hammer and Rubin [1970], it has recently attracted much attention as a way to formulate other CO problems Glover et al. [2022], Lucas [2014], mainly due to the emerging interest in the development of quantum computational devices Boixo et al. [2013], Wang et al. [2013]. By applying simple reformulation techniques, such as constraint penalization Smith et al. [1997], a huge number of CO problems can be formulated as QUBO, which makes algorithms for its solution especially valuable in practice.

Researchers from Amazon Schuetz et al. [2022a] proposed applying GNN to solve QUBO in unsupervised manner, using the differentiable continuous relaxation of Equation 1 as a loss function. This method does not require training data, meaning that GNN is trained to solve the particular problem instance end-to-end, and that it can be considered as autonomous heuristic algorithm. The QUBO matrix is associated with its adjacency graph, on which the GNN is trained. Therefore, such an approach allows using a graph network to solve a wide variety of problems formulated as QUBO, and is not limited to combinatorial problems initially defined on graphs. The main advantage of unsupervised GNNs is the ability to solve very large-scale problems. However, their ability to obtain accurate solutions has been questioned in the community Boettcher [2023], Angelini and Ricci-Tersenghi [2023]: it was claimed that even greedy algorithms outperform GNN. Wang and Li [2023] suggested that it happens because GNNs get stuck in local optima when trained for particular problem instances. To overcome these limitations, we introduce a novel unsupervised QUBO-based Graph Neural Network with a Recurrent Feature (QRF-GNN). The main contribution of our work are as follows:

- We propose a novel GNN architecture QRF-GNN based on a new type of recurrent node connection, which is able to provide accurate solutions for large-scale CO.
- We show that the proposed recurrent design significantly improves the performance of GNNs for all considered types of convolutions.
- We show that our QRF-GNN outperforms existing SOTA learning based approaches for all benchmarks of maximum cut (Max-Cut), graph coloring and maximum independent set (MIS) problems. It also competes with the best existing conventional heuristics, while improving them in scalability and computational time.

2 Proposed QRF-GNN method and Experiment Design

In this section, we first provide a background on graph neural networks and how they are applied to solve QUBO. Then, we describe a new proposed type of recurrent connection for GNNs to enhance their performance on CO. This will be followed by a detailed description of the developed QRF-GNN architecture and a selected set of static features. The last part is devoted to a description of the loss function design for three well-known CO problems on graphs.

2.1 Graph Neural Networks for Combinatorial Optimization

Graph neural networks are capable to learn complex graph-structured data by capturing relational information. During training process, each of the nodes is associated with a vector which is updated based on the information from neighboring nodes.

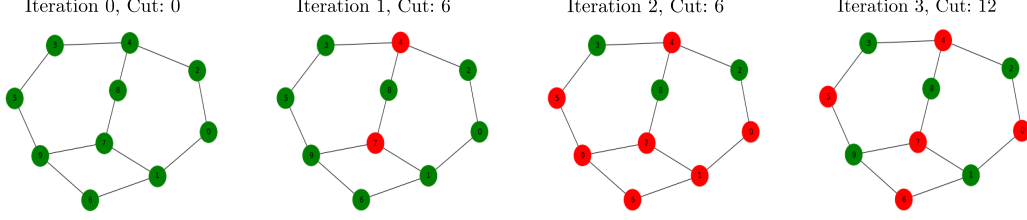


Figure 1: The example of QRF-GNN work on a toy graph of 10 vertices and 12 edges on the Max-Cut problem. The Max-Cut involves partitioning of graph’s nodes into two sets such that the number of edges between sets is maximized. At each iteration, the rounded (discretized) solution is shown: red color refers to $x_i = 0$, green to $x_i = 1$. Using the recurrent feature, QRF-GNN aims to reclassify each node to the opposite class of the majority of its nearest neighbors at each iteration, thereby optimizing the cut. On this instance, QRF-GNN is able to achieve the optimal solution in just a few iterations, while non-recurrent architectures (e.g., PI-GNN) require ~ 50 times more iterations.

Let us consider an undirected graph $G = (V, E)$ with a vertex set $V = \{1, \dots, n\}$ and an edge set $E = \{(i, j) : i, j \in V\}$. Let $h_i^l \in \mathbb{R}^{m_l}$ be a feature vector for a node i and $h_j^l \in \mathbb{R}^{m_l}$ a vector for a node j at the l -th convolution layer and let $e = (i, j)$ be an edge between nodes i and j .

In this paper, we consider GNNs that are based on the message passing protocol to exchange information between nodes. This protocol consists of the two main parts: message accumulation and message aggregation. Message accumulation computes a message m_e^{l+1} for an edge e using a function ϕ , which determines how information will be collected. Message passing includes aggregation of collected messages from a node i neighbors by function ρ and then an update of a feature vector h_i^l for the node i by applying function f with trainable weights W^l . So the whole process is described as follows:

$$m_e^{l+1} = \phi(h_i^l, h_j^l), \quad h_i^{l+1} = f(h_i^l, \rho(\{m_e^{l+1} : (i, j) \in E\})). \quad (2)$$

There are a variety of approaches how to define input features h_i^0 for the node i . It could consist of a one-hot encoding vector of a node label, a random or shared dummy vector Cui et al. [2022], a pagerank Brin and Page [1998] or a degree of a node. It is also possible to use a trainable embedding layer before graph convolutions Schuetz et al. [2022a].

To solve a particular CO problem, Schuetz et al. [2022a] proposed to use the continuous relaxation of the QUBO formulation (Equation 3) as a loss function for GNNs, introducing their physics-inspired GNN (PI-GNN). Replacing the binary decision variables $x_i \in \{0, 1\}$ in Equation 1 with continuous probability parameters $p_i(\theta)$ yields:

$$\mathcal{F}(x) = x^T Q x \rightarrow \mathcal{L}(\theta) = p(\theta)^T Q p(\theta), \quad p(\theta) \in [0, 1]^n, \quad (3)$$

where θ are neural network parameters. After the final N_l -th convolution layer a softmax or sigmoid activation function is applied to compress the final embeddings h^{N_l} into probabilities $p(\theta)$.

As a result of training, GNN obtains the continuous solution $p_i(\theta)$ for each node. In order to obtain a solution of the original discrete problem, $p_i(\theta)$ has to be converted into the discrete variable x_i . The simplest approach is to apply an indicator function $\mathbb{I}_{p_i > p^*}$ with a threshold p^* , as we use in our setup. Alternatively, sampling discrete variables from Bernoulli distribution, or greedy methods can be employed Wang et al. [2022].

2.2 Proposed QRF-GNN Recurrent Framework

Motivation. Existing GNNs often rely solely on the static node features, which can lead to significant limitations. When applying GNNs to solve a specific problem instance, this standard approach can cause the model to become biased towards these features and face node ambiguity issues, resulting in unsupervised GNNs frequently getting trapped in local extrema during training Wang and Li [2023]. Another intuition is related to the QUBO objective 3. It represents the sum of the interaction coefficients of all pairs of non-zero variables. Therefore, the local optimal decision on whether $x_i = 0$ or $x_i = 1$ strongly depends on the classes of the neighbors of node i . Based on these two

considerations, we propose to recursively use the predicted probability data from the previous iteration as an additional dynamic feature of the node, and utilize it directly through the message-passing protocol. Consequently, QRF-GNN operates as an iterative optimization process where nodes update its probabilities based on the probabilities of their nearest neighbors from the previous iteration, aiming to minimize 3. This process is illustrated in Figure 1, which shows the step-by-step work of QRF-GNN on a toy instance for the maximum cut optimization problem. Details of the computational experiment on this graph can be found in Appendix A.6.

Recurrent GNN background. In the regular training process of GNNs, static feature vectors is used as an input to the network, then these vectors are updated through graph convolution layers, after which the loss function is computed and backpropagation with updates of GNN weights occurs. In the previous works, such as Gated Graph Convolution Li et al. [2015] or RUN-CSP Tönshoff J and M [2021], it has been proposed to incorporate recurrence into the GNN training. For this purpose, the LSTM or GRU cell was used to update node hidden and state after message accumulation step, then these vectors are passed back to the input of the convolution layer. The result was a sequence of node states, the length of which is the given hyperparameter of the model. The evolution of states was performed with a fixed matrix of layer weights W^l , taking into account the memory of all previous states. The model weights are updated after the whole sequence is processed, then input vectors are reinitialized with static default values and the next iteration starts.

With these previous approaches, the recurrent update is performed without information about how it affects the loss function. There are also limitations due to the memory propagation of non-optimal previous states which can interfere with the correct abrupt change of the current state, even if this decision is optimal according to the loss function.

Proposed recurrent design. In the QRF-GNN approach, at each iteration $t + 1$ the output state vector h_i^{t, N_i} of the node i from previous iteration t is recurrently used as a dynamic node feature.

Thus, the combination of static a_i and dynamic recurrent features is treated as input of the graph neural network (see Algorithm 1). Model weights are updated according to the loss function at each iteration t , so the matrix W^l at each GNN layer l becomes time dependent $W^{t, l}$ while processing recurrent update. In this design, the sequence of states is not accumulated with a fixed length per iteration as in the RUN-CSP or Gated Graph Convolution, and it is limited only by the number of iterations and convergence criteria. Optimization is performed for the current distribution of node states, and not for the sequence of states changes.

Thus, the neural network can adjust states of nodes with recurrent update to minimize the loss function at each iteration $t + 1$, taking into account the states of neighbors obtained at iteration t and the initial static features of nodes. The proposed method allows to change the current state of a node closer to the optimal one without long-term memory inertia and therefore explore the state space more widely.

Algorithm 1 The QRF-GNN recurrence design

- 1: **Input:** Graph $G(V, E)$, features $\{a_i, \forall i \in V\}$
 - 2: **Output:** Class probabilities $\{p_i, \forall i \in V\}$
 - 3: **for** $t \in \{0, \dots, N_t - 1\}$ **do**
 - 4: **for** $i \in V$ **do**
 - 5: $h_i^{t+1, 0} \leftarrow [a_i, h_i^{t, N_i}]$
 - 6: **end for**
 - 7: **for** $l \in \{0, \dots, N_l - 1\}$ **do**
 - 8: **for** $i \in V$ **do**
 - 9: $h_{N(i)}^{t+1, l+1} \leftarrow \rho \left(\left\{ h_j^{t+1, l}, \forall j \in N(i) \right\} \right)$
 - 10: $h_i^{t+1, l+1} \leftarrow f \left(W^{t, l} [h_i^{t+1, l} \ h_{N(i)}^{t+1, l+1}] \right)$
 - 11: **end for**
 - 12: **end for**
 - 13: $\mathcal{L} \leftarrow \mathcal{L} \left[\sigma \left(\left\{ h_i^{t+1, N_i}, \forall i \in V \right\} \right) \right]$
 - 14: $W^{t+1, l} \leftarrow W^{t, l} - \gamma \nabla_{\theta^l} \mathcal{L}, \forall l$
 - 15: **end for**
 - 16: $\{p_i \leftarrow \sigma(h_i^{N_t, N_t}), \forall i \in V\}$
-

2.3 QRF-GNN Architecture and Training Pipeline

The proposed recurrent framework admits the use of different graph convolution layers. In this work, three options are explored, namely GATv2 Brody et al. [2021], GCN Kipf and Welling [2017] and SAGE Hamilton et al. [2017] convolutional layers. We show that the recurrent connection improves results in all cases, but the SAGE convolution attains better performance and was therefore chosen for the experiments (please see the ablation study 4 for more details).

To improve the representative power of GNNs, we suggest the use of parallel layers, which represents multi-level feature extraction similar to Inception module from computer vision field by Szegedy et al. [2015]. Final architecture of QRF-GNN consists of three SAGE convolutions with different types of aggregation (see Figure 2 and detailed description in Appendix A.1).

Mean and pooling aggregation functions were chosen for two parallel intermediate SAGE layers, and the mean aggregation function was chosen for the last SAGE layer. The pool aggregation allows to determine the occurrence of certain classes among features of neighboring nodes. The mean aggregation shows the ratio of the number of different classes in the neighborhood of the considered node. This architecture configuration with a small number of successive layers allows to store information about local neighborhoods without much over-smoothing Rusch et al. [2023], and its advantages are supported by the ablation study in Appendix B.

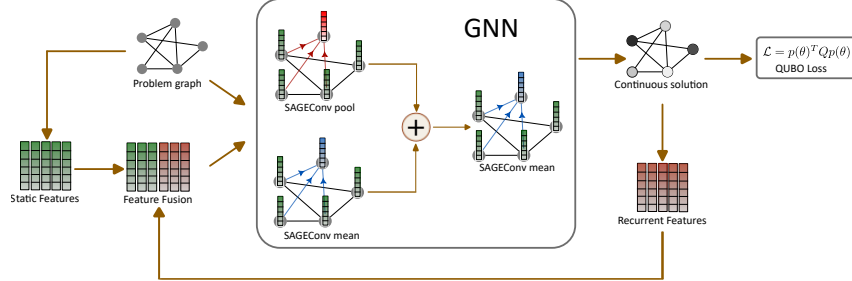


Figure 2: The QRF-GNN architecture. Firstly, the problem graph is associated with the initial QUBO problem, and the node static features are extracted. Then the dynamic recurrent features from the previous iteration is concatenated with the static features. Finally, these fused input vectors along with the graph data pass through the graph neural network to update probabilities p_i in Eq. 3.

As mentioned above, there are several methods how to generate static input features a_i , which then go through a neural network. In this work, we create a static feature vector as a composite vector of a random part, shared vector Cui et al. [2022] and pagerank Brin and Page [1998]. At the first iteration, the probability vector $h_i^{0,0}$ is initialized with zeros. Another way involves one-hot encoding for each node and then training a special embedding layer as in the PI-GNN Schuetz et al. [2022a] architecture. It allows the neural network itself to learn the most representative features. However, we do not use an embedding layer, since it requires additional computational resources and has shown no benefit over artificial features within the framework of conducted experiments (see Appendix B).

2.4 Three Combinatorial Optimization Problems for Our Experiment Design

In this paper focus on three CO problems defined on graphs $G = (V, E)$. It is worth noting that our approach can potentially be applied to any problem that can be formulated as QUBO.

Maximum Cut. The Max-Cut problem involves partitioning the vertices V into two subsets such that the number of edges with endpoints in different subsets is maximized (or the total weight of such edges in the case of a weighted graph). Its QUBO formulation is as follows:

$$\min_{x_i \in \{0,1\}} \mathcal{F}(x) = \sum_{i < j} A_{ij} (2x_i x_j - x_i - x_j), \quad \forall i \in V \quad (4)$$

where A is an adjacency matrix of G . The decision variable $x_i = 1$ indicates that vertex i is in one subset, while $x_i = 0$ indicates that it belongs to another one. In this paper we consider only unweighted graphs with $A_{ij} = 1, \forall (i, j) \in E$.

Graph Coloring. We address two distinct versions of the graph coloring problem. The first one involves coloring a graph $G = (V, E)$ using a predetermined number of colors to minimize the number of adjacent vertices sharing the same color, thereby avoiding violations. The second formulation seeks to determine the minimum number of colors required to color the graph without violations. The QUBO formulations of both coloring problems is formulated as follows:

$$\min_{x_{i,c} \in \{0,1\}} \mathcal{F}(x) = \sum_i \left(1 - \sum_c x_{i,c} \right)^2 + \sum_{(i,j) \in E} \sum_c x_{i,c} x_{j,c}, \quad \forall i \in V, \forall c \in \{1, \dots, k\}, \quad (5)$$

where k is the number of colors the graph has to be colored. For the second coloring problem k is not fixed. The loss function can be reduced to the second term of the objective 5 in order to train QRF-GNN or PI-GNN. The condition for the uniqueness of the color assigned to the node which is specified by the first term is met automatically by the softmax layer.

Maximum Independent Set.

For a given graph $G = (V, E)$ the Maximum Independent Set (MIS) problem is to find a subset $S \subset V$ of pair-wise nonadjacent nodes of the maximum size $|S|$. The QUBO formulation of MIS is as follows:

$$\min_{x_i \in \{0,1\}} \mathcal{F}(x) = - \sum_{i \in V} x_i + P \sum_{(i,j) \in E} x_i x_j \quad \forall i \in V. \quad (6)$$

where $x_i = 1$ if node $i \in S$ and P is a penalty coefficient for violating the independence condition, which ensures that no two adjacent nodes are both included in the independent set. Unlike the previously considered problems, this formulation contains a penalty term, raising the question of which value of P should be chosen. In our algorithm an adaptive coefficient was applied. For more details, please see Appendix A.5.

3 Numerical experiments

In this section, we experimentally evaluated the performance of the algorithm on three popular combinatorial optimization problems, namely maximum cut, maximum independent set and graph coloring. The benchmark data included both generated random graphs and well-known graphs of various structures of synthetic and real-world origin. We selected the best among learning algorithms and classical heuristics for each CO problem to compare the results.

We found out that there was no need to do a time-consuming optimization of QRF-GNN hyperparameters (as it is done in the PI-GNN algorithm) to overcome existing GNNs. However, the hyperparameters tuning may lead to better results of QRF-GNN. The only parameters that we changed for different problems were the size of hidden layers and the maximum number of iterations, since for some types of graphs fewer iterations were sufficient to get a competitive result. As the solution to which the algorithm converges depends on the initialization, it is preferable to do multiple runs with different seeds to get the best result. We provide a detailed description of the experimental setup in Appendix A.1.

3.1 Maximum Cut

To evaluate the performance of QRF-GNN, we compared results with other GNNs and popular heuristics on randomly generated regular graphs and the synthetic dataset Gset by Ye [2003].

Table 1: P -value of EO, PI-GNN, RUN-CSP and QRF-GNN for d -regular graphs with 500 nodes and different degree d averaged over 200 randomly generated instances.

d	HEUR	UNSUPERVISED LEARNING		
	EO	PI-GNN	RUN-CSP	QRF-GNN
3	0.727	0.612	0.714	0.725
5	0.737	0.608	0.726	0.738
10	0.735	0.658	0.710	0.737
15	0.736	0.644	0.697	0.739
20	0.732	0.640	0.685	0.735

For the synthetic data the number of cut edges was counted as a metric.

For random regular graphs with the number of vertices $n \rightarrow \infty$, there exists a theoretical estimate of the maximum cut size that depends on n , vertex degree d and a universal constant $P_* \simeq 0.7632$. Such asymptotics led to the appearance of a metric which is calculated as $P\text{-value} = \sqrt{\frac{4}{d}} \left(\frac{z}{n} - \frac{d}{4} \right)$, where z corresponds to the obtained cut size (see Yao et al. [2019]).

A higher P -value corresponds to a better cut, and the closer it is to P_* , the nearer the solution found is to the best possible.

Table 1 shows the mean over 200 graphs P -value obtained with specialized extremal optimization heuristics (EO) by Boettcher [2003], RUN-CSP and QRF-GNN for random regular graphs with $n = 500$ nodes and different degrees d . For QRF-GNN and PI-GNN we present results for the best value out of 5 runs. The PI-GNN architecture with

GCN layers and setup as in Schuetz et al. [2022a] was used for the calculations on graphs with $d > 5$, other values are taken from the original paper. Results of EO and RUN-CSP were presented by Tönshoff J and M [2021], where RUN-CSP was allowed to make 64 runs for each graph. QRF-GNN clearly outperforms RUN-CSP and PI-GNN in all cases and starting from $d = 5$ shows the best results over all considered algorithms. Increasing the number of runs to 15 allows QRF-GNN to show the best result on graphs with $d = 3$ with P -value = 0.727.

Table 2 contains the comparison results on Gset of our algorithm with PI-GNN, RUN-CSP, EO and the SOTA heuristics Breakout Local Search (BLS) by Benlic and Hao [2013] and the Tabu Search based Hybrid Evolutionary Algorithm (TSHEA) by Wu et al. [2015]. To obtain the data, the τ -EO heuristic was implemented according to Boettcher and Percus [2001] (details in A.3 in the appendix).

QRF-GNN as well as BLS and TSHEA was run 20 times on each graph and the best attempt out of 64 was chosen for RUN-CSP. For the results of PI-GNN, the authors applied intensive hyperparameter optimization for each graph separately (see Schuetz et al. [2022a]). Our algorithm outperforms both neural network approaches and the EO heuristic. Compared to the SOTA heuristics, QRF-GNN finds fewer cut edges on most small graphs, but on the largest presented graph G70 it not only yields the best number of cuts, but also requires only ~ 1000 s, while BLS and TSHEA took several times more, or about ~ 11000 s and ~ 7000 s correspondingly (see Benlic and Hao [2013], Wu et al. [2015]).

Table 2: Number of cut edges for benchmark instances from Gset Ye [2003] with the number of nodes $|V|$ and the number of edges $|E|$. QRF-GNN outperforms all other GNN-based approaches and the EO heuristic, while being comparable to SOTA heuristics.

GRAPH	$ V $	$ E $	HEURISTICS			UNSUPERVISED LEARNING		
			BLS	TSHEA	EO	PI-GNN	RUN-CSP	QRF-GNN
G14	800	4694	3064	3064	3058	3026	2943	3058
G15	800	4661	3050	3050	3046	2990	2928	3049
G22	2000	19990	13359	13359	13323	13181	13028	13340
G49	3000	6000	6000	6000	6000	5918	6000	6000
G50	3000	6000	5880	5880	5878	5820	5880	5880
G55	5000	12468	10294	10299	10212	10138	10116	10282
G70	10000	9999	9541	9548	9433	9421	9319	9559

3.2 Graph Coloring

We performed experiments on synthetic graphs from the COLOR dataset Trick [2002] and additional calculations for three real-world citation graphs Cora, Citeseer and Pubmed Li et al. [2022]. While the number of vertices in synthetic graphs ranged from 25 and 561, citation graphs contained up to about 20 thousand vertices. The detailed specifications can be found in Appendix A.4.

Results of graph coloring are compared with other GNN-based architectures, such as PI-GNN by Schuetz et al. [2022b], GNN-1N by Wang et al. [2023], GDN by Li et al. [2022] and RUN-CSP by Tönshoff J and M [2021], and the SOTA heuristics HybridEA by Galinier and Hao [1999]. The code¹ which was used for the HybridEA estimation is based on Lewis [2021]. To evaluate the results of QRF-GNN, we did up to 10 runs for some graphs, although most of them required only one run.

Table 3 shows the best result of algorithms for coloring a graph with a chromatic number of colors. A violation occurs if there are adjacent vertices of the same color in the graph. It can be seen that QRF-GNN shows the best results on all instances, even outperforming the results of the SOTA heuristic on some graphs.

Table 4 shows the number of colors that the algorithm needs to color the graph without violations. Since the authors of GNN-1N and GDN do not obtain results for this problem formulation in the original papers, we omitted them and compared additionally with RUN-CSP. For QRF-GNN, we successively increased the number of colors to find the optimal one. In this problem formulation, QRF-GNN also surpasses existing GNN-based solutions, and is inferior to the HybridEA heuristics on only one graph.

¹<http://rhydlewislewis.eu/gcol/>

Table 3: The number of violations when coloring the graph with chromatic number of colors by HybridEA (HEA) heuristics and GNN-based methods GNN-IN, PI-GNN, GDN and QRF-GNN for citation graphs and graphs from the COLOR dataset.

GRAPH	HEUR	UNSUPERVISED LEARNING			
	HEA	GNN-IN	PI-GNN	GDN	QRF-GNN
HOMER	0	0	0	0	0
MYCIEL6	0	0	0	0	0
QUEEN5-5	0	0	0	0	0
QUEEN6-6	0	0	0	0	0
QUEEN7-7	0	0	0	9	0
QUEEN8-8	0	1	1	-	0
QUEEN9-9	0	1	1	-	0
QUEEN8-12	0	0	0	0	0
QUEEN11-11	14	13	17	21	7
QUEEN13-13	18	15	26	33	15
CORA	0	1	0	0	0
CITSEER	0	0	0	0	0
PUBMED	0	-	17	21	0

Table 4: The number of color needed for coloring without violations by HybridEA (HEA) heuristics and GNN-based methods PI-GNN, RUN-CSP and QRF-GNN on citation graphs and graphs from the COLOR dataset. Here χ is a known chromatic number.

GRAPH	χ	HEUR	UNSUPERVISED LEARNING		
		HEA	PI-GNN	RUN-CSP	QRF-GNN
HOMER	13	13	13	17	13
MYCIEL6	7	7	7	8	7
QUEEN5-5	5	5	5	5	5
QUEEN6-6	7	7	7	8	7
QUEEN7-7	7	7	7	10	7
QUEEN8-8	9	9	10	11	9
QUEEN9-9	10	10	11	17	10
QUEEN8-12	12	12	12	17	12
QUEEN11-11	11	12	14	>17	12
QUEEN13-13	13	14	17	>17	15
CORA	5	5	5	-	5
CITSEER	6	6	6	-	6
PUBMED	6	8	9	-	8

3.3 Maximum Independent Set

For MIS, we conduct experiments on randomly generated graphs of different structures. The results shown in Table 5 represents a comparison of QRF-GNN with the range of cutting edge learning-based algorithms on two sets of Erdos-Renyi (ER) random graphs of 700-800 vertices and 9000-11000 vertices of 500 graphs each (see Erdos and Rényi [1984]).

Table 5: Comparison of average found MIS sizes and runtime for QRF-GNN, learning-based methods and the SOTA heuristics KamIS on sets of 500 Erdos-Renyi random graphs with a different number of nodes.

METHOD	TYPE	ER-[700-800]		ER-[9000-11000]	
		SIZE	TIME	SIZE	TIME
KAMIS	HEUR	44.87	52:13	374.57	7:37:21
INTEL	SL	34.86	6:04	284.63	5:02
DIFUSCO	SL	40.35	32:98	-	-
T2TCO	SL	41.37	29:44	-	-
LwD	RL	41.17	6:33	345.88	1:02:29
DIMES	RL	42.06	12:01	332.8	12:31
GFLowNETS	UL	41.14	2:55	349.42	1:49:43
QRF-GNN	UL	42.45	3:46	375.44	10:32

to solve large problems from the ER-9000-11000 dataset (see Zhang et al. [2023]), we omitted their results. As can be seen from Table 5, QRF-GNN performs the best among all learning methods. This is especially evident on large graphs, where it surpasses the results of Kamis, being significantly superior in terms of speed.

We also follow Tönshoff J and M [2021] and make experiments on a collection of hard instances with hidden optimal solutions generated by the RB model Xu and Li [2006] (see Table 6). In this case, QRF-GNN outperforms both RUN-CSP and greedy baselines, and is slightly inferior to KamIS.

Table 6: MIS results of QRF-GNN, GNN-based method RUN-CSP, greedy and SOTA KamIS heuristics on RB Model graphs. We report average MIS sizes over 5 runs with standard deviations.

GRAPH	V	E	HEURISTICS		UNSUPERVISED LEARNING	
			KAMIS	GREEDY	RUN-CSP	QRF-GNN
FRB30-15	450	18K	30 ± 0.0	24.6 ± 0.5	25.8 ± 0.8	28.4 ± 0.4
FRB40-19	790	41K	39.4 ± 0.5	33.0 ± 1.2	33.6 ± 0.5	36.8 ± 0.7
FRB50-23	1150	80K	48.8 ± 0.4	42.2 ± 0.8	42.2 ± 0.4	45 ± 0.6
FRB59-26	1478	126K	57.4 ± 0.9	48.0 ± 0.7	49.4 ± 0.5	54.6 ± 1

4 Impact of the recurrence connection on GNNs performance.

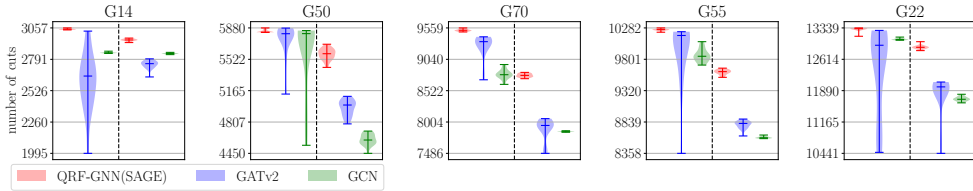


Figure 3: Distribution of the results over 20 runs of GNNs with different convolutional layers with (left) and without (right) recurrent connection on several instances from Gset. Horizontal lines mean maximum, median and minimum values.

We have investigated how the recurrent use of vertex class membership affects architectures with different types of convolutions, namely GCN Kipf and Welling [2017] and GATv2 Brody et al. [2021] in addition to the default architecture of QRF-GNN with SAGE convolutions. For this purpose, we constructed GNNs from two consecutive convolutions of a given type. The sizes of hidden states were the same for all networks and coincided with the sizes of the described default QRF-GNN architecture. We performed 20 calculations with different seeds for graphs from Gset to solve the Max-Cut problem. Figure 3 shows that the type of recurrence proposed in this paper greatly improves the maximum cut found for all types of convolutions. At the same time, the default QRF-GNN shows better results compared to other architectures.

5 Related work

Graph neural networks are rapidly gaining popularity as a powerful tool for solving CO problems Cappart et al. [2023]. Supervised learning based approaches are commonly applied Prates et al. [2019], Li et al. [2018b], Gasse et al. [2019], Li et al. [2018a], Sun and Yang [2023], Li et al. [2023]. However, the need to collect labeled training instances into representative and unbiased dataset is a significant limitation of supervised algorithms. Additionally, they often face challenges with generalization to new, unseen problem instances. Reinforcement learning (RL) presents an alternative by generating iterative solutions Mazyavkina et al. [2021], Khalil et al. [2017], Kool et al. [2019], Qiu et al. [2022]. While being promising approach, reinforcement learning methods may experience difficulties when facing large scale problems due to the vastness of the state space, and the need of a large number of samplings. The unsupervised learning paradigm, where solvers do not require a training set of pre-solved problems, has the potential to overcome these limitations. Tönshoff J and M [2021] proposed RUN-CSP as a recurrent GNN to solve maximum constraint satisfaction. Amizadeh et al. [2018] developed GNN to solve SAT and CircuitSAT. Karalias and Loukas [2020] train GNN to obtain a distribution of nodes corresponding to the candidate solution and Sun et al. [2023] provided an annealed version of it. Wang et al. [2022] study entry-wise concave relaxations of CO objectives. Schuetz et al. [2022a] apply relaxed QUBO as instance specific GNN loss, Schuetz et al. [2022b], Wang et al. [2023] extend it for solving graph coloring problem.

6 Conclusion

In this work, we propose the novel recurrent algorithm QRF-GNN for graph neural networks, designed for solving combinatorial optimization problems in unsupervised mode. We show that our novel recurrent feature update method significantly enhances the performance of all types of GNN convolutions considered. We conduct computational experiments on the well-known maximum cut, graph coloring and maximum independent set problems. The results of our comparative analysis demonstrate that QRF-GNN drastically outperforms all learning-based baselines, including SOTA supervised, unsupervised, and reinforcement learning methods. Moreover, we show that QRF-GNN competes with the best classical heuristics for the problems addressed while showing a distinct advantage in computational time on large graphs.

For the future work, we consider QRF-GNN superior performance and scalability promising to be extended to other CO problem formulated as QUBO, thus highlighting its potential in the field of combinatorial optimization.

References

- Ilhem Boussaïd, Julien Lepagnot, and Patrick Siarry. A survey on optimization metaheuristics. *Information Sciences*, 237:82–117, 2013. ISSN 0020-0255. doi: <https://doi.org/10.1016/j.ins.2013.02.041>. URL <https://www.sciencedirect.com/science/article/pii/S0020025513001588>. Prediction, Control and Diagnosis using Advanced Neural Computations.
- Quentin Cappart, Didier Chételat, Elias Khalil, Andrea Lodi, Christopher Morris, and Petar Veličković. Combinatorial optimization and reasoning with graph neural networks. *Journal of Machine Learning Research*, 24(130):1–61, 2023. URL <http://jmlr.org/papers/v24/21-0449.html>.
- Peter L. Hammer and Sergiu Rudeanu. Pseudo-boolean programming. *Operations Research*, 17(2): 233–261, 1969. ISSN 0030364X, 15265463. URL <http://www.jstor.org/stable/168831>.
- Endre Boros and Peter L. Hammer. The max-cut problem and quadratic 0–1 optimization; polyhedral aspects, relaxations and bounds. *Annals of Operations Research*, 33:151–180, 1991.
- Peter L. Hammer and Abraham A. Rubin. Some remarks on quadratic programming with 0-1 variables. 1970. URL <https://api.semanticscholar.org/CorpusID:53617855>.
- Fred Glover, Gary Kochenberger, Rick Hennig, and Yu Du. Quantum bridge analytics i: a tutorial on formulating and using QUBO models. *Annals of Operations Research*, 314(1):141–183, April 2022. doi: [10.1007/s10479-022-04634-2](https://doi.org/10.1007/s10479-022-04634-2). URL <https://doi.org/10.1007/s10479-022-04634-2>.
- Andrew Lucas. Ising formulations of many NP problems. *Frontiers in Physics*, 2, 2014. doi: [10.3389/fphy.2014.00005](https://doi.org/10.3389/fphy.2014.00005). URL <https://doi.org/10.3389/fphy.2014.00005>.
- Sergio Boixo, Tameem Albash, Federico M. Spedalieri, Nicholas Chancellor, and Daniel A. Lidar. Experimental signature of programmable quantum annealing. *Nature Communications*, 4(1), June 2013. ISSN 2041-1723. doi: [10.1038/ncomms3067](https://doi.org/10.1038/ncomms3067). URL <http://dx.doi.org/10.1038/ncomms3067>.
- Zhe Wang, Alireza Marandi, Kai Wen, Robert L. Byer, and Yoshihisa Yamamoto. Coherent ising machine based on degenerate optical parametric oscillators. *Phys. Rev. A*, 88:063853, Dec 2013. doi: [10.1103/PhysRevA.88.063853](https://doi.org/10.1103/PhysRevA.88.063853). URL <https://link.aps.org/doi/10.1103/PhysRevA.88.063853>.
- Alice E Smith, David W Coit, Thomas Baeck, David Fogel, and Zbigniew Michalewicz. Penalty functions. *Handbook of evolutionary computation*, 97(1):C5, 1997.
- Martin J. A. Schuetz, J. Kyle Brubaker, and Helmut G. Katzgraber. Combinatorial optimization with physics-inspired graph neural networks. *Nature Machine Intelligence*, 4(4):367–377, April 2022a. doi: [10.1038/s42256-022-00468-6](https://doi.org/10.1038/s42256-022-00468-6). URL <https://doi.org/10.1038/s42256-022-00468-6>.
- Stefan Boettcher. Inability of a graph neural network heuristic to outperform greedy algorithms in solving combinatorial optimization problems. *Nature Machine Intelligence*, 5(1):24–25, January 2023. doi: [10.1038/s42256-022-00587-0](https://doi.org/10.1038/s42256-022-00587-0). URL <https://doi.org/10.1038/s42256-022-00587-0>.
- Maria Chiara Angelini and Federico Ricci-Tersenghi. Modern graph neural networks do worse than classical greedy algorithms in solving combinatorial optimization problems like maximum independent set. *Nature Machine Intelligence*, 5(1):29–31, January 2023. doi: [10.1038/s42256-022-00589-y](https://doi.org/10.1038/s42256-022-00589-y). URL <https://doi.org/10.1038/s42256-022-00589-y>.
- Haoyu Peter Wang and Pan Li. Unsupervised learning for combinatorial optimization needs meta learning. 2023. URL <https://openreview.net/forum?id=-ENYHCE8zBp>.
- Hejie Cui, Zijie Lu, Pan Li, and Carl Yang. On positional and structural node features for graph neural networks on non-attributed graphs. In *Proceedings of the 31st ACM International Conference on Information & Knowledge Management, CIKM '22*, page 3898–3902, New York, NY, USA, 2022. Association for Computing Machinery. ISBN 9781450392365. doi: [10.1145/3511808.3557661](https://doi.org/10.1145/3511808.3557661). URL <https://doi.org/10.1145/3511808.3557661>.

- Sergey Brin and Lawrence Page. The anatomy of a large-scale hypertextual web search engine. *Computer Networks and ISDN Systems*, 30(1):107–117, 1998. ISSN 0169-7552. doi: [https://doi.org/10.1016/S0169-7552\(98\)00110-X](https://doi.org/10.1016/S0169-7552(98)00110-X). URL <https://www.sciencedirect.com/science/article/pii/S016975529800110X>. Proceedings of the Seventh International World Wide Web Conference.
- Haoyu Peter Wang, Nan Wu, Hang Yang, Cong Hao, and Pan Li. Unsupervised learning for combinatorial optimization with principled objective relaxation. 2022. URL https://openreview.net/forum?id=HjNn9oD_v47.
- Yujia Li, Daniel Tarlow, Marc Brockschmidt, and Richard Zemel. Gated graph sequence neural networks. 2015.
- Wolf H Tönshoff J, Ritzert M and Grohe M. Graph neural networks for maximum constraint satisfaction. *Frontiers in Artificial Intelligence*, 3, 2021. doi: 10.3389/frai.2020.580607. URL <https://doi.org/10.3389/frai.2020.580607>.
- Shaked Brody, Uri Alon, and Eran Yahav. How attentive are graph attention networks? *arXiv preprint arXiv:2105.14491*, 2021.
- Thomas N. Kipf and Max Welling. Semi-supervised classification with graph convolutional networks, 2017.
- William L. Hamilton, Rex Ying, and Jure Leskovec. Inductive representation learning on large graphs. In *Proceedings of the 31st International Conference on Neural Information Processing Systems, NIPS'17*, page 1025–1035, Red Hook, NY, USA, 2017. Curran Associates Inc. ISBN 9781510860964.
- Christian Szegedy, Wei Liu, Yangqing Jia, Pierre Sermanet, Scott Reed, Dragomir Anguelov, Dumitru Erhan, Vincent Vanhoucke, and Andrew Rabinovich. Going deeper with convolutions. In *2015 IEEE Conference on Computer Vision and Pattern Recognition (CVPR)*, pages 1–9, 2015. doi: 10.1109/CVPR.2015.7298594.
- T. Konstantin Rusch, Michael M. Bronstein, and Siddhartha Mishra. A survey on oversmoothing in graph neural networks. *ArXiv*, abs/2303.10993, 2023. URL <https://api.semanticscholar.org/CorpusID:257632346>.
- Y. Ye. The G-set dataset, 2003. URL <https://web.stanford.edu/~yye/yye/Gset/>.
- Weichi Yao, Afonso S. Bandeira, and Soledad Villar. Experimental performance of graph neural networks on random instances of max-cut. In Dimitri Van De Ville, Manos Papadakis, and Yue M. Lu, editors, *Wavelets and Sparsity XVIII*, volume 11138, page 111380S. International Society for Optics and Photonics, SPIE, 2019. doi: 10.1117/12.2529608. URL <https://doi.org/10.1117/12.2529608>.
- S. Boettcher. Numerical results for ground states of spin glasses on Bethe lattices. *The European Physical Journal B - Condensed Matter*, 31(1):29–39, January 2003. doi: 10.1140/epjb/e2003-00005-y. URL <https://doi.org/10.1140/epjb/e2003-00005-y>.
- Una Benlic and Jin-Kao Hao. Breakout local search for the max-cut problem. *Engineering Applications of Artificial Intelligence*, 26(3):1162–1173, 2013. ISSN 0952-1976. doi: <https://doi.org/10.1016/j.engappai.2012.09.001>. URL <https://www.sciencedirect.com/science/article/pii/S0952197612002175>.
- Qinghua Wu, Yang Wang, and Zhipeng Lü. A tabu search based hybrid evolutionary algorithm for the max-cut problem. *Applied Soft Computing*, 34:827–837, 2015. ISSN 1568-4946. doi: <https://doi.org/10.1016/j.asoc.2015.04.033>. URL <https://www.sciencedirect.com/science/article/pii/S1568494615002604>.
- Stefan Boettcher and Allon G. Percus. Optimization with extremal dynamics. *Physical Review Letters*, 86(23):5211–5214, June 2001. doi: 10.1103/physrevlett.86.5211. URL <https://doi.org/10.1103/physrevlett.86.5211>.
- M. Trick. Color dataset, 2002. URL <https://mat.tepper.cmu.edu/COLOR02/>.

- Wei Li, Ruxuan Li, Yuzhe Ma, Siu On Chan, David Pan, and Bei Yu. Rethinking graph neural networks for the graph coloring problem. *ArXiv*, abs/2208.06975, 2022.
- Martin J. A. Schuetz, J. Kyle Brubaker, Zhihuai Zhu, and Helmut G. Katzgraber. Graph coloring with physics-inspired graph neural networks. *Phys. Rev. Res.*, 4:043131, Nov 2022b. doi: 10.1103/PhysRevResearch.4.043131. URL <https://link.aps.org/doi/10.1103/PhysRevResearch.4.043131>.
- Xiangyu Wang, Xueming Yan, and Yaochu Jin. A graph neural network with negative message passing for graph coloring, 2023.
- Philippe Galinier and Jin-Kao Hao. Hybrid evolutionary algorithms for graph coloring. *Journal of Combinatorial Optimization*, 3:379–397, 01 1999. doi: 10.1023/A:1009823419804.
- R. Lewis. *Guide to Graph Colouring: Algorithms and Applications*. 01 2021. ISBN 978-3-030-81053-5. doi: 10.1007/978-3-030-81054-2.
- Paul L. Erdos and Alfréd Rényi. On the evolution of random graphs. *Transactions of the American Mathematical Society*, 286:257–257, 1984. URL <https://api.semanticscholar.org/CorpusID:6829589>.
- Zhuwen Li, Qifeng Chen, and Vladlen Koltun. Combinatorial optimization with graph convolutional networks and guided tree search. In *Neural Information Processing Systems*, 2018a. URL <https://api.semanticscholar.org/CorpusID:53027872>.
- Zhiqing Sun and Yiming Yang. DIFUSCO: Graph-based diffusion solvers for combinatorial optimization. In *Thirty-seventh Conference on Neural Information Processing Systems*, 2023. URL <https://openreview.net/forum?id=JV8Ff0lgVW>.
- Yang Li, Jinpei Guo, Runzhong Wang, and Junchi Yan. From distribution learning in training to gradient search in testing for combinatorial optimization. In *Thirty-seventh Conference on Neural Information Processing Systems*, 2023. URL <https://openreview.net/forum?id=JtF0ugNMv2>.
- Sungsoo Ahn, Younggyo Seo, and Jinwoo Shin. Learning what to defer for maximum independent sets. In *Proceedings of the 37th International Conference on Machine Learning, ICML'20*. JMLR.org, 2020.
- Ruizhong Qiu, Zhiqing Sun, and Yiming Yang. DIMES: A differentiable meta solver for combinatorial optimization problems. In *Advances in Neural Information Processing Systems 35*, 2022.
- Dinghui Zhang, Hanjun Dai, Nikolay Malkin, Aaron Courville, Yoshua Bengio, and Ling Pan. Let the flows tell: Solving graph combinatorial problems with GFlownets. In *Thirty-seventh Conference on Neural Information Processing Systems*, 2023. URL <https://openreview.net/forum?id=sTjW3JHs2V>.
- Sebastian Lamm, Peter Sanders, Christian Schulz, Darren Strash, and Renato F. Werneck. Finding near-optimal independent sets at scale. *Journal of Heuristics*, 23(4):207–229, May 2017. ISSN 1572-9397. doi: 10.1007/s10732-017-9337-x. URL <http://dx.doi.org/10.1007/s10732-017-9337-x>.
- Ke Xu and Wei Li. Many hard examples in exact phase transitions. *Theoretical Computer Science*, 355(3):291–302, 2006. ISSN 0304-3975. doi: <https://doi.org/10.1016/j.tcs.2006.01.001>. URL <https://www.sciencedirect.com/science/article/pii/S0304397506000181>.
- Marcelo Prates, Pedro H. C. Avelar, Henrique Lemos, Luis C. Lamb, and Moshe Y. Vardi. Learning to solve np-complete problems: A graph neural network for decision tsp. *Proceedings of the AAAI Conference on Artificial Intelligence*, 33(01):4731–4738, Jul. 2019. doi: 10.1609/aaai.v33i01.33014731. URL <https://ojs.aaai.org/index.php/AAAI/article/view/4399>.
- Z. Li, Q. Chen, and V. Koltun. Combinatorial optimization with graph convolutional networks and guided tree search. page 537–546, 2018b.

- Maxime Gasse, Didier Chételat, Nicola Ferroni, Laurent Charlin, and Andrea Lodi. Exact combinatorial optimization with graph convolutional neural networks. In *Advances in Neural Information Processing Systems 32*, 2019.
- Nina Mazyavkina, Sergey Sviridov, Sergei Ivanov, and Evgeny Burnaev. Reinforcement learning for combinatorial optimization: A survey. *Computers & Operations Research*, 134:105400, 2021. ISSN 0305-0548. doi: <https://doi.org/10.1016/j.cor.2021.105400>. URL <https://www.sciencedirect.com/science/article/pii/S0305054821001660>.
- Elias B. Khalil, Hanjun Dai, Yuyu Zhang, Bistra Dilikina, and Le Song. Learning combinatorial optimization algorithms over graphs. In Isabelle Guyon, Ulrike von Luxburg, Samy Bengio, Hanna M. Wallach, Rob Fergus, S. V. N. Vishwanathan, and Roman Garnett, editors, *Advances in Neural Information Processing Systems 30: Annual Conference on Neural Information Processing Systems 2017, December 4-9, 2017, Long Beach, CA, USA*, pages 6348–6358, 2017. URL <https://proceedings.neurips.cc/paper/2017/hash/d9896106ca98d3d05b8cbdf4fd8b13a1-Abstract.html>.
- Wouter Kool, Herke van Hoof, and Max Welling. Attention, learn to solve routing problems! In *International Conference on Learning Representations*, 2019. URL <https://openreview.net/forum?id=ByxBFsRqYm>.
- Saeed Amizadeh, Sergiy Matuselych, and Markus Weimer. Learning to solve circuit-sat: An unsupervised differentiable approach. In *International Conference on Learning Representations*, 2018. URL <https://api.semanticscholar.org/CorpusID:53544639>.
- Nikolaos Karalias and Andreas Loukas. Erdos goes neural: an unsupervised learning framework for combinatorial optimization on graphs. In H. Larochelle, M. Ranzato, R. Hadsell, M.F. Balcan, and H. Lin, editors, *Advances in Neural Information Processing Systems*, volume 33, pages 6659–6672. Curran Associates, Inc., 2020. URL https://proceedings.neurips.cc/paper_files/paper/2020/file/49f85a9ed090b20c8bed85a5923c669f-Paper.pdf.
- Haoran Sun, Etash Kumar Guha, and Hanjun Dai. Annealed training for combinatorial optimization on graphs, 2023. URL <https://openreview.net/forum?id=YHCR6CFAK6v>.
- Martin J. A. Schuetz, J. Kyle Brubaker, and Helmut G. Katzgraber. Reply to: Inability of a graph neural network heuristic to outperform greedy algorithms in solving combinatorial optimization problems. *Nature Machine Intelligence*, 5(1):26–28, January 2023. doi: 10.1038/s42256-022-00588-z. URL <https://doi.org/10.1038/s42256-022-00588-z>.

A Technical Details and Convergence

A.1 General experimental setup

All random graphs in this work were generated by the NetworkX² package. To implement the QRF-GNN architecture the DGL library³ was used. The pseudocode of one iteration with the QRF-GNN architecture is presented in the Algorithm 2. We used the Adam optimizer without a learning rate schedule. The learning rate was set empirically to 0.014, the rest of the optimizer parameters remained set by default. Gradients were clipped at values 2 of the Euclidean norm.

We limited the number of iterations to 5×10^4 for random regular graphs and 10^5 for all the other graphs, but in some cases convergence was reached much earlier. If the value of the loss function at the last 500 iterations had differed by less than 10^{-5} it was decided that the convergence was achieved and the training was stopped. In the case of the graph coloring problem, an additional stopping criterion was used and the solution was considered to be found when the absolute value of the loss function becomes less than 10^{-3} .

The dropout was set to 0.5. The dimension of the random part of input vectors was equal to 10, the size of hidden layers was fixed at 50 for Max-Cut and at 140 for graph coloring.

Due to the stochasticity of the algorithm, it is preferable to do multiple runs with different seeds to find the best result. One can do separate runs in parallel possibly utilizing several GPUs. If the device has enough memory, the RUN-CSP scheme by Tönshoff J and M [2021] can be used. In this case, one composite graph with duplicates of the original one is created for the input. We trained the model in parallel on the NVIDIA Tesla V100 GPU. Conventional heuristics were launched on the machine with two Intel Xeon E5-2670 v3 @ 2.30GHz.

We tested three ways to recursively utilize the probability data. Specifically, we passed raw probability data taken before the sigmoid layer, data after the sigmoid layer or concatenated both of these options. Different recurrent features led to a minor improvement on some graphs, while at the same time slightly worsening the results on other graphs. In this work we presented results for the concatenated data.

Algorithm 2 Forward propagation of the QRF-GNN algorithm at iteration t

- 1: **Input:** Graph $G(V, E)$, static nodes features $\{a_i, \forall i \in V\}$
 - 2: **Output:** Probability p_i , hidden state $h_i^t, \forall i \in V$
 - 3: $h_i^{t,0} \leftarrow [a_i, h_i^{t-1}], \quad \forall i \in V$
 - 4: **for** $i \in V$ **do**
 - 5: $h_{N(i)}^{t,1} \leftarrow \rho_{\text{mean}} \left(\left\{ h_j^{t,0}, \forall j \in N(i) \right\} \right)$
 - 6: $h_i^{t,1} \leftarrow f \left(W^1 [h_i^{t,0}, h_{N(i)}^{t,1}] \right)$
 - 7: $h_{N(i)}^{t,2} \leftarrow \rho_{\text{pool}} \left(\left\{ h_j^{t,0}, \forall j \in N(i) \right\} \right)$
 - 8: $h_i^{t,2} \leftarrow f \left(W^2 [h_i^{t,0}, h_{N(i)}^{t,2}] \right)$
 - 9: **end for**
 - 10: $\{h_i^{t,1}\} \leftarrow \text{BN}_{\gamma_1, \beta_1}(\{h_i^{t,1}, \forall i \in V\})$
 - 11: $\{h_i^{t,2}\} \leftarrow \text{BN}_{\gamma_2, \beta_2}(\{h_i^{t,2}, \forall i \in V\})$
 - 12: **for** $i \in V$ **do**
 - 13: $h_i^{t,12} \leftarrow f(h_i^{t,1} + h_i^{t,2})$
 - 14: $h_i^{t,12} \leftarrow \text{Dropout}(h_i^{t,12})$
 - 15: $h_{N(i)}^{t,\text{out}} \leftarrow \rho_{\text{mean}} \left(\left\{ h_j^{t,12}, \forall j \in N(i) \right\} \right)$
 - 16: $h_i^{t,\text{out}} \leftarrow f \left(W^{\text{out}} [h_i^{t,12}, h_{N(i)}^{t,\text{out}}] \right)$
 - 17: **end for**
 - 18: $p_i, h_i^t \leftarrow \sigma(h_i^{t,\text{out}}), h_i^{t,\text{out}}, \quad \forall i \in V$
-

²<https://networkx.org/>

³<https://www.dgl.ai/>

A.2 Convergence

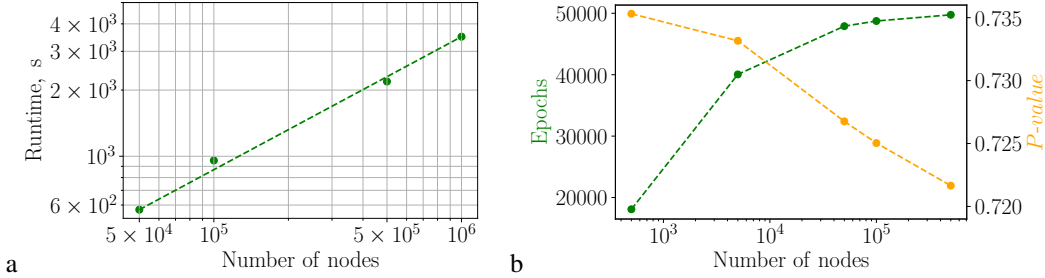


Figure 4: a) The computation time of 5×10^4 iterations of QRF-GNN on random regular graphs with $d = 5$ in the sparse format depending on the number of nodes. b) The iteration number averaged over 20 graphs at which the algorithm found the best solution during the training process (green) and the mean P -value for 1 run (orange).

The number of runs and iterations in experiments were not optimal and were chosen for a more fair comparison with other algorithms. More runs and iterations can lead to better results. We conducted additional experiments on 20 random regular graphs with $d = 5$ and up to one million nodes. One run was made for each graph and the number of iterations was limited to 5×10^4 . The training time for large graphs in sparse format on single GPU is shown in Figure 4a. We also analyzed how the number of iterations can affect the quality of the solution. As the number of vertices increases, the iteration at which the last found best solution was saved moves closer to the specified boundary (see Figure 4b). Meanwhile, the average P -value of one run drops from 0.735 to 0.722 and one of the reasons for this may include the limited duration of training. If, for example, we train QRF-GNN for 10^5 iterations on graphs with $n = 5 \times 10^4$ nodes, the average P -value will increase from 0.726 to 0.728, while on small graphs with $n = 500$ we do not observe such an effect. Thus, it is difficult to talk about the convergence of the algorithm on large instances under the given constraint. The recommendation is to follow the latest best solution updates and terminate the algorithm if it does not change for a sufficiently large ($> 10^4$) number of iterations.

In order to study the robustness of the algorithm with respect to changes in hyperparameters, we run the default QRF-GNN architecture with two parallel layers on graphs from the Gset dataset for the Max-Cut problem. All hyperparameters except the learning rate were chosen as described in Section 3. As can be seen from Figure 5, small values of the learning rate do not allow to achieve convergence in 10^5 iterations. For the learning rate greater than 0.01 the results become relatively stable and the best number of cuts is achieved for values from 0.01 to 0.02.

A.3 Max-Cut

In Table 1 results of EO and RUN-CSP were taken from Tönshoff J and M [2021], where P -value was averaged over 1000 graphs. RUN-CSP was allowed to make 64 runs for each graph and in the case of EO the best of two runs was chosen Yao et al. [2019]. P -values of PI-GNN depend on the particular architecture. Results for graphs with a degree 3 and 5 were published in Schuetz et al. [2022a] for the architecture with GCN layer, and it corresponds to the value in the column for PI-GNN. The cut size was bootstrap-averaged over 20 random graph instances and PI-GNN took up to 5 shots. In the paper by Schuetz et al. [2023] the authors considered another option with the SAGE layer and showed that in this case the results for graphs with a degree 3 can be improved by 10.78%. However, we did not notice an improvement over the GCN architecture on graphs with a higher degree.

To make the evaluation more informative, we implemented τ -EO heuristic from Boettcher and Percus [2001]. As suggested by authors, we set $\tau = 1.3$ and the number of single spin updates was limited by 10^7 . For small graphs τ -EO can find a high-quality solution, but with increase of the graph size the accuracy of the algorithm degrades due to the limited number of updates. This behavior is expected by the authors, who suggested optimal scaling for number of updates as $\sim O(|V|^3)$. However, it is computationally expensive to carry out the required number of iterations. We performed 20 runs of EO with different initializations to partially compensate for this. Within the given limit, the EO algorithm took ~ 6800 seconds per run to obtain a solution for the relatively large graph G70.

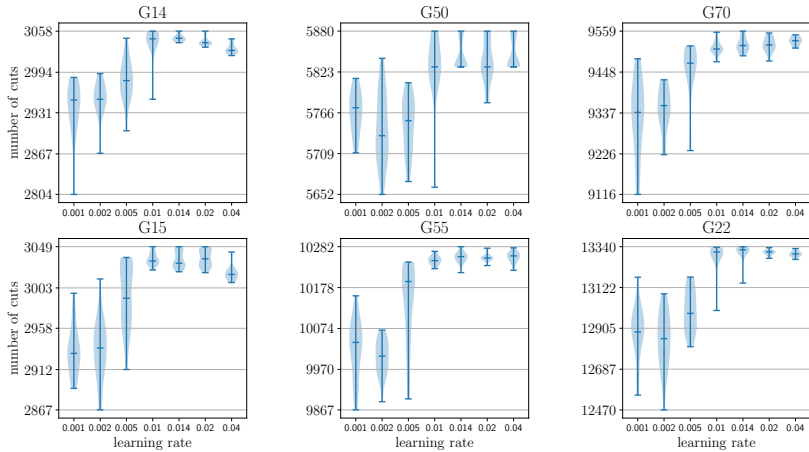


Figure 5: Results distribution for 20 runs of the default QRF-GNN architecture depending on the learning rate for the Max-Cut problem on several instances from Gset. The number of iterations in all cases was fixed at 10^5 . Horizontal lines mean maximum, median and minimum values.

QRF-GNN as well as BLS and TSHEA was run 20 times on each graph. The best attempt out of 64 was chosen for RUN-CSP in original papers. In order to obtain the results of PI-GNN, the authors applied hyperparameter optimization for each graph. The results of RUN-CSP for the G70 graph was obtained by running the code⁴ with parameters reported in Tönshoff J and M [2021].

A.4 Coloring

To find the number of colors required to color the graph without violations, we successively increased the number of colors in each new run until the correct coloring was found among 10 seeds. The number of nodes and edges of the investigated graphs is presented in Table 8. To evaluate the results of QRF-GNN, we did up to 10 runs for some graphs, although most of them required only one run. The convergence time for PI-GNN and QRF-GNN is shown in Table 7.

Results for graphs *anna*, *david*, *games120*, *muciel5*, *huck* and *jean* were omitted in the main tables because all algorithms find optimal solutions without violations. Results of GNN-1N for citation graphs were obtained by implementing the algorithm from the original paper. Since there was no instruction how to optimize hyperparameters, we took them close to PI-GNN and chose the best among 10 runs.

The number of iterations for convergence of QRF-GNN on citation graphs was no more than 6000 and varied for the COLOR dataset from ~ 200 to 9×10^4 . The estimated runtime for QRF-GNN turned out to be significantly less than for PI-GNN, and in some cases the difference reaches more than three orders of magnitude. This is due to the fact that QRF-GNN does not require exhaustive tuning of hyperparameters for each instance in contrast to PI-GNN Schuetz et al. [2022b].

Table 7: Approximate runtime in seconds for PI-GNN and QRF-GNN training on a single GPU on instances from the COLOR dataset and citation graphs.

Graph	$ V $	$ E $	PI – GNN, $\times 10^3$ s	QRF – GNN, $\times 10^3$ s
COLOR	25-561	160-3328	$3.6 \div 28.8$	$0.002 \div 1$
CORA	2708	5429	0.3	0.06
CITeseer	3327	4732	2.4	0.018
PUBMED	19717	44338	24	0.156

⁴<https://github.com/toenshoff/RUN-CSP>

Table 8: Number of Vertices and Edges in coloring graphs.

Graph	$ V $	$ E $
ANNA	138	493
DAVID	87	406
GAMES120	120	638
HOMER	561	1629
HUCK	74	301
JEAN	80	254
MYCIEL5	47	236
MYCIEL6	95	755
QUEEN5-5	25	160
QUEEN6-6	36	290
QUEEN7-7	49	476
QUEEN8-8	64	728
QUEEN9-9	81	1056
QUEEN8-12	96	1368
QUEEN11-11	121	1980
QUEEN13-13	169	3328
CORA	2708	5429
CITeseer	3327	4732
PUBMED	19717	44338

A.5 MIS

In our experiments, we found that setting a small P leads to the fact that the solutions found by the algorithm for a given number of iterations contain too many violations. A large P value can cause the algorithm to quickly converge to a trivial solution with zero set size. To circumvent the problem of adjusting P for different types of graphs, we propose in this paper to linearly increase the penalty value from 0.01 to 2 throughout all the iterations. This allows the algorithm to start the search in the space of large sets with violations while gradually narrowing the search space towards sets without violations.

A.6 Toy example of a Max-Cut problem

We provide a toy example of a Max-Cut problem to illustrate the performance of our proposed QRF-GNN method compared to the PI-GNN approach. The problem instance consists of a graph with 12 edges and 10 nodes, as shown in Figure 1.

An experimental setup for the QRF-GNN architecture is set by default similar to the description in section 3. The PI-GNN architecture consists of a trainable embedding layer and one hidden layer, the sizes of which are set similarly to QRF-GNN and equal to 50.

For the considered problem, QRF-GNN finds the optimal solution (cut = 12) in an average of 10.96 iterations, while PI-GNN requires 532.1 iterations on average. These results are based on 100 runs with different random seeds.

B Ablation for QRF-GNN Components

We analyzed which components of QRF-GNN make the greatest contribution to its performance on the example of Max-Cut problem-solving. The default architecture includes two intermediate SAGEConv layers and the recurrent feature. The most dramatic drop in quality occurs if the recurrent part is excluded (see Figure 7).

Throwing out one of the intermediate convolutional layer does not result in such a strong downgrade (see Figure 8). However, the absence of the convolutional layer with a pool aggregation function leads to a decrease in the median result, upper bound, and an increase in the results dispersion for almost all graphs. Discarding the layer with a mean aggregation function can increase the median cut and even decrease the variance in some cases, but upper bounds either stay the same or decrease, even if we double the number of parameters in the remaining hidden layer (see Figure 8). Further ablation on random regular graphs shows that the absence of any convolutional layer leads to a worse result (see Figure 9). Table 9 with average results for one seed and the best of the five seeds also confirms the advantage of using a combination of two layers.

In this work, we settled on combining a random vector, shared vector Cui et al. [2022] and pagerank Brin and Page [1998] for the input feature vector by default. Fig. 6 shows the results when one of the parts (random vectors or the pagerank of nodes) was removed. In some cases, the median improves after dropping features, but the upper bound tends to only go down as the number of input features decreases. Using an embedding layer does not show any benefit over the default version.

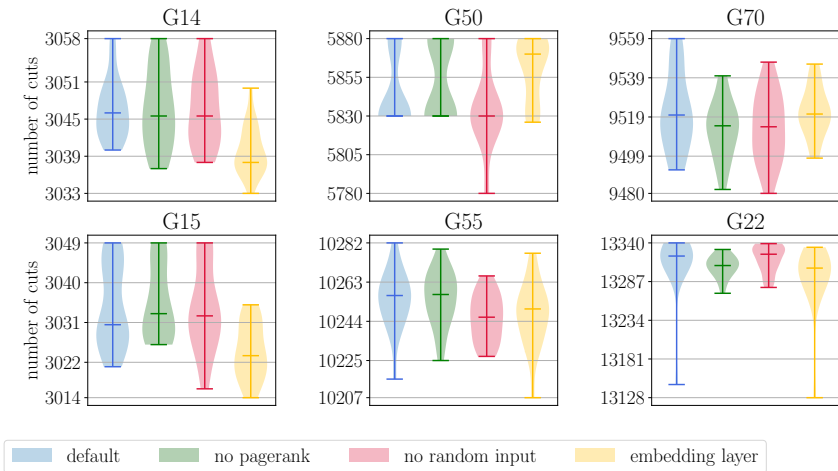


Figure 6: Results distribution for 20 runs of QRF-GNN with the default architecture on several instances from Gset. Input feature vectors varied as follows: the default choice corresponds to the blue color; the exclusion of the pagerank component corresponds to the green color; the exclusion of the random part corresponds to the red color. The use of a trainable embedding layer instead of artificial features is indicated in yellow.

Table 9: The first row contains the average P -value over 200 random regular graphs with $d = 5$ for 1 run of QRF-GNN with same configurations as in Figures 8 and 9. The second row shows the average P -value over 200 graphs when the best cut out of 5 runs is taken.

Runs	Default	no SAGEConv (mean)	no SAGEConv (pool)
1	0.734	0.732	0.725
5	0.738	0.737	0.734

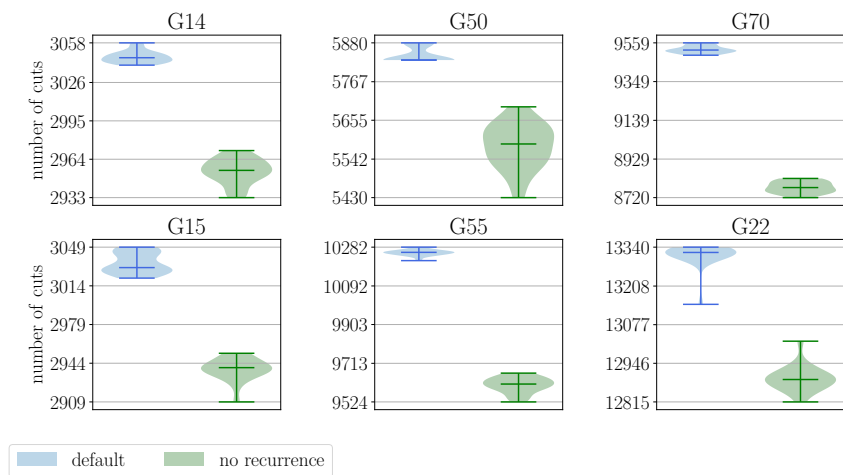


Figure 7: Results distribution for 20 runs of QRF-GNN with (blue) and without (green) the recurrent connection on several instances from Gset. Horizontal lines mean maximum, median and minimum values.

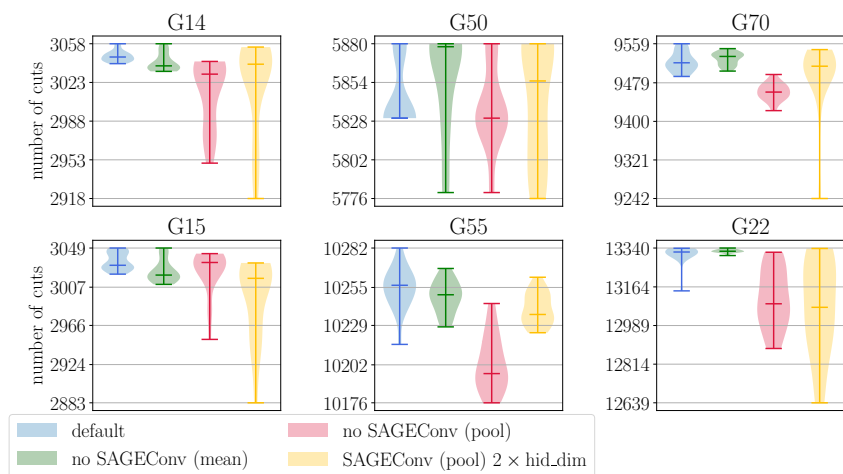


Figure 8: Results distribution for 20 runs of QRF-GNN of the default architecture (blue), with the absence of one SAGE layer with a mean aggregation function (green) or the SAGE layer with a pool aggregation function (red). Horizontal lines mean maximum, median and minimum values.

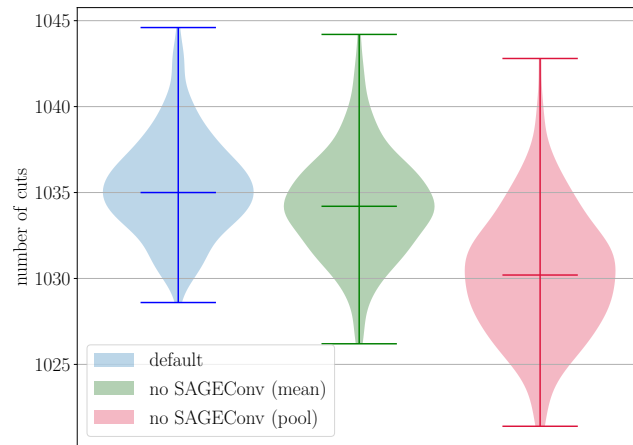


Figure 9: Results distribution for the mean of 5 runs on 200 random regular graphs with $d = 5$ and 500 nodes. QRF-GNN had the same configurations as in the Fig. 8.